Biogeosciences Discuss., 6, 8609–8631, 2009
www.biogeosciences-discuss.net/6/8609/2009/

Biogeosciences Discussions

Biogeosciences Discussions is the access reviewed discussion forum of *Biogeosciences*

Assessment of soil *n*-alkane δD and branched tetraether membrane lipid distributions as tools for paleoelevation reconstruction

F. Peterse[1], M. T. J. van der Meer[1], S. Schouten[1], G. Jia[2], J. Ossebaar[3], J. Blokker[1], and J. S. Sinninghe Damsté[1,3]

[1]Department of Marine Organic Biogeochemistry, NIOZ Royal Netherlands Institute for Sea Research, P.O. Box 59, 1790 AB Den Burg, Texel, The Netherlands
[2]State Key Laboratory of Organic Geochemistry, Guangzhou Institute of Geochemistry, Chinese Academy of Sciences, Guangzhou 510640, China
[3]Faculty of Geosciences, Utrecht University, P.O. Box 80021, 3508 TA Utrecht, The Netherlands

Received: 21 August 2009 – Accepted: 25 August 2009 – Published: 1 September 2009

Correspondence to: F. Peterse (francien.peterse@nioz.nl)

Published by Copernicus Publications on behalf of the European Geosciences Union.

Abstract

$\delta^{18}O$ values of pedogenic minerals forming from soil water are commonly used to reconstruct paleoelevation. To circumvent some of the disadvantages of this method, soil *n*-alkane δD values were recently proposed as a new tool to reconstruct elevation changes, after showing that soil *n*-alkane δD values track the altitude effect on precipitation δD variations (r^2=0.73 along Mt. Gongga, China). To verify the suitability of soil *n*-alkane δD values as a paleoelevation proxy we measured the δD of soil *n*-alkanes along Mt. Kilimanjaro (Tanzania). At midslope, soil *n*-alkane δD values are highly influenced by the present precipitation belt, causing D-depletion. Consequently, soil *n*-alkane δD values do not linearly relate with altitude (r^2=0.03), suggesting that they can not serve as an unambiguous proxy to infer past elevation changes. In contrast, it was recently shown that the MBT/CBT temperature proxy, which is based on the distribution of branched glycerol dialkyl glycerol tetraether (GDGT) membrane lipids, is linearly related with MAT, and thus altitude (r^2=0.77), at Mt. Kilimanjaro. This suggests that this proxy may be more suitable for paleoelevation reconstruction. However, application of the MBT/CBT proxy on the altitude gradient along Mt. Gongga showed that, although the MBT/CBT-derived temperature lapse rate (−5.9°C/1000 m) resembles the measured temperature lapse rate (−6.0°C/1000 m), there is a relatively large degree of scatter (r^2=0.55). Our results thus show that both proxies can be subject to relatively large uncertainties in their assessment of past elevation changes, but that a combination of the soil *n*-alkane δD and MBT/CBT proxies can likely result in a more reliable assessment of paleoelevation.

1 Introduction

Stable isotope values of authigenic and pedogenic minerals are a common tool for the reconstruction of paleoelevation changes in mountain ranges (e.g. Poage and Chamberlain, 2001; Rowley and Garzione, 2007, and references therein). $\delta^{18}O$ and δD

BGD

6, 8609–8631, 2009

values of precipitation and meteoric water become more negative with increasing elevation due to rain-out caused by the decrease in temperature and relative humidity, the so-called "altitude effect" (Dansgaard, 1964), a trend that has been recognized in almost all mountain belts of the world (Poage and Chamberlain, 2001). The present day stable oxygen isotope composition of precipitation or meteoric water is well documented in e.g. authigenic carbonates or soil water. This relationship can be used to infer elevation changes of mountain ranges (e.g. Poage and Chamberlain, 2001; Rowley and Garzione, 2007, and references therein). Precipitation and surface water isotopic composition along an altitude gradient provides an isotopic lapse rate that can be used as a reference line for the reconstruction of historical elevation changes. By comparing the reference line with the isotopic values of pedogenic minerals that have formed in the past, such as carbonates, clays, or volcanic glass that, at the time of formation, have formed in equilibrium with surface waters, a paleoelevation record can be obtained. However, there are some disadvantages in using this method. For example, the obtained records are generally very smoothed due to the low formation rate of carbonates, and show a millennial signal at best (Rowley and Garzione, 2007). Furthermore, the mineral isotopic composition can be influenced by different source waters and temperature variations during formation (Dettman and Lohmann, 2000; Rowley and Garzione, 2007). Also, diagenesis and recrystallization can modify the original isotopic composition of pedogenic minerals (Morrill and Koch, 2002; Garzione et al., 2004). Thus, further development of paleoelevation proxies is needed to reduce uncertainties in paleoelevation reconstructions, including developing and validating new proxies, and combining these different proxies in multi-proxy applications.

Recently, Jia et al. (2008) explored the suitability of soil *n*-alkane δD values as a proxy for paleoelevation as it has been shown previously that hydrogen isotope ratios of leaf wax *n*-alkanes strongly relate to that of environmental water values (e.g. Sessions et al., 1999; Sauer et al., 2001; Sachse et al., 2004; Smith and Freeman, 2006; Rao et al., 2009) and that the hydrogen isotopic composition of environmental water depends on altitude (Dansgaard, 1964). Indeed, the *n*-alkane δD values for surface

soils along the eastern slope of Mt. Gongga (China) record the altitude effect on the precipitation δD well, showing a decreasing trend with altitude (Jia et al., 2008). An advantage of using *n*-alkanes hydrogen isotope values instead of those of pedogenic minerals, is that elevations can also be determined at sites where no carbonates are present, but where organic material has been preserved. Furthermore, the production of plant lipids is a relatively short-term process compared to the formation and precipitation of minerals, which makes it possible to increase the resolution of the paleoelevation records. Finally, the uncertainties from the temperature effect during mineral formation that has to be taken into account when using mineral isotope values (Poage and Chamberlain, 2001) can be largely avoided by the use *n*-alkane δD data, as the isotopic fractionation between water and plant lipids during lipid production is seemingly less temperature dependent than that during carbonate precipitation (Jia et al., 2008). However, a disadvantage of this proxy is that the isotopic fractionation may be influenced by physical or vegetation changes along an altitudinal transect, so that soil *n*-alkane δD values can only be applied as a paleoelevation proxy when hydrogen isotope fractionation between precipitation and plant wax *n*-alkanes appears to be independent of elevation, or when changes in fractionation can be reconstructed (Jia et al., 2008).

An alternative method to reconstruct paleoelevation could be the MBT/CBT temperature proxy, which is based on the membrane composition of a yet unknown group of bacteria that occurs ubiquitously in soils worldwide (Weijers et al., 2007c). The membranes of these bacteria are composed of branched glycerol dialkyl glycerol tetraether (GDGT; Fig. 1) lipids, of which the molecular structure can vary in the amount of methyl branches (4 to 6) attached to the alkyl chain, and in the number of cyclopentane moieties (up to 2) (Sinninghe Damsté et al., 2000; Weijers et al., 2006). An empirical study showed that the amount of cyclopentane moieties linearly relates with soil pH, whereas the degree of methylation shows a relation with both soil pH and annual mean air temperature (MAT; Weijers et al., 2007c). These relations are expressed in two indices, the Cyclisation of Branched Tetraether (CBT) and the Methylation of Branched Tetraether

(MBT) index. By analyzing the distribution of branched GDGTs, which can be determined from the same lipid extract as used for *n*-alkane δD measurements, and using the combination of the CBT and MBT indices, changes in past environmental conditions can be reconstructed (Weijers et al., 2007a, b; Schouten et al., 2008). Sinninghe Damsté et al. (2008) showed that the distributions of branched GDGTs in surface soils from Mt. Kilimanjaro (Tanzania) change with temperature, and thus with altitude, despite variations in precipitation or soil type. The temperature lapse rate that was calculated using the MBT/CBT proxy (−6.9±1.0°C/1000 m; Sinninghe Damsté et al., 2008), approached the lapse rate that was measured in situ (−5.3°C/1000 m; Hemp, 2006b). Branched GDGTs are generally well preserved, and have been found in sediments as old as the Palaeocene-Eocene thermal maximum (~55 Ma; Weijers et al., 2007b), suggesting that they may be suitable components for paleoelevation studies, when applied to paleosols, for example.

Here, we apply both soil *n*-alkane δD values and the MBT/CBT proxy on two altitudinal transects to test their suitability for paleoelevation reconstructions. Soil *n*-alkane δD values were measured along the slope of Mt. Kilimanjaro, and the MBT/CBT temperature proxy was applied along the slope of Mt. Gongga. The same samples were previously analyzed for the MBT/CBT proxy of Mt. Kilimanjaro soils and for soil *n*-alkane δD analysis of Mt. Gongga by Sinninghe Damsté et al. (2008) and Jia et al. (2008), respectively.

2 Material and methods

2.1 Altitudinal transects and soil samples

Mt. Kilimanjaro is located 300 km south of the equator in Tanzania on the border with Kenya (3° S, 37° E). Mt. Kilimanjaro is an ancient volcano, rising from the 700 m elevated savanna plains to a height of 5895 m, which makes it the highest mountain in Africa. Precipitation and temperature vary with altitude and the degree of exposure to

wind from the Indian Ocean. Annual precipitation is higher on the southern slope than on the northern slope.

Due to its location close to the equator Mt. Kilimanjaro experiences two distinct rainy seasons; long rains from March to May, and short, but heavy rains in November and December (Hemp, 2006a, b). Rainfall data for the southern slope show an increase in precipitation from about 1900 mm/y at 1400 m to a maximum of about 2700 mm/y at 2200 m altitude, and then decreasing again towards 50% of the maximum rainfall at 3000 m, and only 20% at 4000 m (Hemp, 2006a, b). MAT is 23.4°C at about 800 m, and decreases linearly upslope with a lapse rate of −5.3°C/1000 m to a MAT of −7.1°C at the top (Hemp, 2006b). Also the vegetation on Mt. Kilimanjaro shows a zonated pattern along the slope (Hemp, 2006a, b). Soil *n*-alkane δD analysis were performed on the same soils as used by Sinninghe Damsté et al. (2008), who sampled 16 surface soils between 1700 m and 3300 m along the southeastern slope of Mt. Kilimanjaro in September 2006. The soil pH for this altitudinal transect ranges from 3.8 to 6.6 (Hemp, 2006b).

Mt. Gongga (7556 m) is located in the Daxue Mountain Range on the eastern side of the Tibetan plateau in Sichuan Province, southwest China (30° N, 102° E). The eastern slope of Mount Gongga drops 6450 m in altitude in only 29 km horizontal distance into the Dadu River valley at 1100 m, the western slope blends into the Tibetan Plateau at 3000–3500 m (Thomas, 1997). Climate characteristics for the eastern and western side of the mountain are substantially different; the east side is influenced by Pacific air masses, whereas the west side is under influence of the Southwest Monsoon. This results in a relatively cool and humid climate with heavy precipitation on the east side of the mountain, and a drier and warmer climate on the west side. Annual precipitation increases with altitude on both sides, with the major part falling during the hottest summer months (May to October) (Thomas, 1997, 1999). Weather station data show that MAT declines upward from 11.8°C at 1600 m to 3.4°C at 3000 m (Jia et al., 2008). The climatic changes along the altitudinal gradient cause variations in soil and vegetation types, showing a vertical zonated pattern along the slope (Thomas, 1999; Zhong et

al., 1999). The soils used for branched GDGT analysis are similar to the ones used in Jia et al. (2008). Our sample set comprises of 36 surface horizons (0–5 cm) along an altitude gradient from 1180 m to 3819 m on the eastern slope of Mt. Gongga, and was sampled in late May 2004. The soils were stored frozen upon arrival in the laboratory in China, and freeze dried before shipping to the laboratory at NIOZ. The pH of the soils was measured in the laboratory in China in a 1:2.5 soil:water (w/v) mixture.

2.2 Soil extractions

All soils were freeze dried and powdered with mortar and pestle prior to extraction (3 times for 5 min) with a solvent mixture of dichloromethane (DCM):MeOH (9:1, v/v) using an accelerated solvent extractor (ASE 200, Dionex) at 100°C and 7.6×10^6 Pa. Each total extract was dried using a rotary evaporator under near vacuum. The extracts were dissolved in DCM and passed over a Na_2SO_4 column to remove all remaining water, dried again under a N_2 flow, and weighed, depending on which 0.1–1.0 µg of a C_{46} GDGT standard was added to the extracts (cf. Huguet et al., 2006). The extracts were separated by passing them over an activated Al_2O_3 column using hexane:DCM (9:1, v/v) and DCM:MeOH (1:1, v/v) to obtain an apolar and polar fraction, respectively.

2.2.1 Soil *n*-alkane δD analysis

The apolar fractions were each passed over a small silver nitrate impregnated silica column using hexane to further separate the *n*-alkanes. The *n*-alkane containing fractions were analyzed by gas chromatography (GC) using an Agilent 6890 gas chromatograph with a flame ionization detector using a fused silica capillary column (25 m×0.32 mm) coated with CP Sil-5 (film thickness=0.12 µm) with helium as carrier gas. The fractions were dissolved in *n*-hexane, and injected on-column at 70°C. The oven was programmed to subsequently increase the temperature to 130°C with 20°C/min, and then with 4°C/min to 320°C at which it was held isothermal for 10 min. Compound-specific hydrogen isotopic compositions of the *n*-alkanes were determined by GC/thermal con-

version/isotope ratio monitoring mass spectrometer using a Thermo Electron DELTA-Plus XL mass spectrometer. GC conditions were similar to conditions for GC analysis except that the film thickness of the CPSil 5 column was 0.4 µm and that a constant flow of He was used at 1.5 ml/min. Compounds were pyrolyzed at 1450°C in an empty ceramic tube, which was preactivated by a methane flow of 0.5 ml/min for 5 min. H_3^+-factors were determined daily on the isotope mass spectrometer and varied between 6 and 8.5. H_2 gas with known isotopic composition was used as reference and a mixture of C_{16}–C_{32} *n*-alkanes of known isotopic composition (ranging from −42‰ to −256‰ vs. VSMOW) was used to monitor the performance of the system. The average offsets between the measured hydrogen isotopic composition of the C_{16}–C_{32} *n*-alkanes and their values determined off-line were generally 5‰ or less. Analyses were done at least in duplicate and the reproducibility was always better than 7‰. A squalane standard was co-injected with every sample and its average value was −170.6±3.5‰, which compared favorably with its off-line determined value of −170‰.

δD values for precipitation (δD_p) along the slope of Mt. Kilimanjaro were calculated according to Bowen and Revenaugh (2003) and Bowen (2009), and given in Table 1.

Isotope fractionation between precipitation (δD_p) and plant wax *n*-alkanes (δD_{wax}) is expressed as fractionation factor α, where:

$$\alpha = \frac{(1000 + \delta D_{wax})}{(1000 + \delta D_p)} . \quad (1)$$

2.2.2 Branched GDGT analysis

The polar fractions, containing the branched GDGTs, were dried under N_2, ultrasonically dissolved in a hexane:isopropanol (99:1, v/v) mixture, and filtered over a 0.45 µm PTFE filter. All polar fractions were concentrated to about 3 mg/ml prior to analysis by high performance liquid chromatography/atmospheric pressure chemical ionization-mass spectrometry (HPLC/APCI-MS) on an Agilent 1100 series LC/MSD SL according to Schouten et al. (2007), with minor modifications. Briefly, separation of the branched

GDGTs was achieved on an Alltech Prevail Cyano column (150 mm×2.1 mm; 3 µm). The compounds were eluted isocratically with 90% A and 10% B for 5 min (flow rate 0.2 ml/min), and then with a linear gradient to 16% B for 34 min, where A=hexane and B=hexane:isopropanol (9:1, v/v). For all samples, the injection volume was 10 µl. Selective ion monitoring of the $[M+H]^+$ was used to detect and quantify the different GDGTs, and absolute quantification of each compound was achieved by calculating the area of its corresponding peak in the chromatogram, comparing it with the peak area of the internal standard, and correcting it for the different response factors (cf. Huguet et al., 2006).

The CBT and MBT indices were calculated according to the following equations:

$$\mathrm{CBT} = -\log\left(\frac{[\mathrm{Ib} + \mathrm{IIb}]}{[\mathrm{Ia} + \mathrm{IIa}]}\right), \quad (2)$$

$$\mathrm{MBT} = \frac{[\mathrm{Ia} + \mathrm{Ib} + \mathrm{Ic}]}{[\mathrm{Ia} + \mathrm{Ib} + \mathrm{Ic} + \mathrm{IIa} + \mathrm{IIb} + \mathrm{IIc} + \mathrm{IIIa} + \mathrm{IIIb} + \mathrm{IIIc}]}. \quad (3)$$

Roman numerals refer to the structures in Fig. 1. The soil pH and MAT were calculated using the empirical equations based on the global calibration set given by (Weijers et al., 2007c):

$$\mathrm{CBT} = 3.33 - 0.38 \times \mathrm{pH}, \quad (4)$$

$$\mathrm{MBT} = 0.122 + 0.187 \times \mathrm{CBT} + 0.020 \times \mathrm{MAT}. \quad (5)$$

Average errors based on duplicate analysis for MBT and CBT on 12 samples are 0.003 and 0.007, respectively.

3 Results and discussion

3.1 Soil *n*-alkane δD values along Mt. Kilimanjaro

Soil *n*-alkanes along Mt. Kilimanjaro range from C_{27} to C_{35}, and are dominated by odd-over-even *n*-alkanes, as is represented by the carbon preference index (CPI) of

the *n*-alkanes, which ranges from 5.5 to 15.8 (Table 1). The average chain length (ACL) of the C_{27}–C_{35} *n*-alkanes along the analyzed transect varies between 30.2 and 32.0 (Table 1). C_{29}, C_{31}, and C_{33} *n*-alkanes are most abundant in the soils, and their hydrogen isotope values range from −154‰ to −126‰ for the C_{29}, from −149‰ to −113‰ for the C_{31}, and from −144‰ to −116‰ for the C_{33} *n*-alkane (Table 1).

To test if the δD of higher plant *n*-alkanes on Mt. Kilimanjaro records precipitation δD, we plotted the weighed mean of the δD of the most common *n*-alkanes (C_{29}, C_{31} and C_{33}; δD_{wax}) against the modeled δD_p (Bowen and Revenaugh, 2003) and altitude, similar to the approach followed by Jia et al. (2008) (Fig. 2a, b). This shows that δD_{wax} values do not strongly correlate with the modeled δD_p, as was found for Mt. Gongga (Jia et al., 2008). Indeed, the fractionation factor α is not constant with altitude but apparently increases with altitude except for altitudes <1800 m (Fig. 2c). Changes in vegetation could be one cause for the apparent different fractionations with altitude. The forest on the lower slope of Mt. Kilimanjaro is dominated by the angiosperm *Ocotea*, which has its main habitat in the middle montane zone, where humidity is at its maximum, as indicated by a wealth of ferns (Hemp, 2006b). From 2500 m on *Ocotea* is taken over by the gymnosperm *Podocarpus* (Hemp, 2006b). The change from an angiosperm to a more gymnosperm dominated forest can also be seen in the ACL of the *n*-alkanes along Mt. Kilimanjaro (Fig. 2d), as the $ACL_{(27-35)}$ is in general distinct for angiosperm and gymnosperm leaf waxes (29.4 and 33.0, respectively; Rommerskirchen et al., 2006). Thus, the change in vegetation from angiosperm to gymnosperm could potentially explain the different fractionations observed with altitude. However, Chikaraishi and Naraoka (2003) found that the hydrogen isotopic composition of angiosperms leaf wax *n*-alkanes was not significantly different from that of gymnosperm *n*-alkanes of various terrestrial plants in Japan and Thailand. In contrast, studies by Pedentchouk et al. (2007, 2008) found that gymnosperm tree leaf wax *n*-alkanes were depleted in *D* relative to those of the angiosperm trees. However, the δD_{wax} values for Mt. Kilimanjaro show an opposite trend to what would be expected based on the shift in vegetation, and, thus, the change in apparent fractionation is

BGD
6, 8609–8631, 2009

unlikely to be explained by the changing vegetation.

Alternatively, the lack of correlation between δD_{wax} and modeled δD_p may be because the modeled δD_p does not reflect the actual δD_p at the sampling sites. The isotopic composition of precipitation, and thus of δD_{wax}, is related with the temperature at which condensation takes place, but for this transect along Mt. Kilimanjaro condensation temperature can not explain the observed depletion in δD_{wax}, as the air temperature along the slope linearly decreases with altitude, with no apparent deviations along the slope (Hemp, 2006a, b). The amount of precipitation and relative humidity, however, reach their maximum in the middle montane zone (Hemp, 2006a, b), exactly where δD_{wax} values are most depleted and the apparent fractionation factors the largest. It has previously been observed that in tropical regions the isotopic composition of precipitation is not only related to the condensation temperature, but mainly controlled by local rainout, which is known as the "amount effect" (Rozanski et al., 1992; Rozanski and Araguás Araguás, 1995). This "amount effect" results in more depleted δD_p values with higher amounts of rainfall and/or harder rains. The "amount effect" is not yet well understood due to the numerous atmospheric processes that are involved in obtaining the final isotopic composition of precipitation, although convective activity and re-evaporation seem to be the major influence (Vimeux et al., 2005; Risi et al., 2008a, b). Nevertheless, this "amount effect" might shift the actual δD_p at the midslope high precipitation belt to much lower values than the modeled δD_p. Indeed, along the western slope of Mt. Kenya (0° S, 37° E), which has a climate similar to Mt. Kilimanjaro, precipitation and lake water δD values were also found to be influenced by the "amount effect" rather than by the "altitude effect" (Rietti-Shati et al., 2000).

Another possibility is that the actual fractionation between δD_p and δD_{wax} is higher at this midslope high precipitation belt than downslope en upslope. According to Smith and Freeman (2006), the apparent fractionation between δD_p and δD_{wax} mainly depends on humidity. Higher humidity results in less evaporative enrichment of leaf water δD, and therefore a higher apparent fractionation between δD_p and δD_{wax}. The increase in humidity and precipitation in the middle montane zone as mentioned by

BGD
6, 8609–8631, 2009

Hemp (2006a, b) could therefore result in a more depleted actual δD_p than modeled, as well as a higher apparent fractionation. This combined effect thus could mask the relationship between δD_{wax} on the one hand and δD_p or altitude at the other (Fig. 2a, b).

3.2 Branched GDGTs along Mt. Gongga

Branched GDGTs were found in all analyzed surface soils of Mt. Gongga. Their concentrations vary between 0.01 and 5.3 µg/g dry weight (dwt) soil (Table 2). The distribution of branched GDGTs varies substantially, as is reflected by the CBT and MBT indices, which were calculated according to Eq. (2) and Eq. (3), respectively (Table 2). The CBT index for the soils ranges from 0.03 to 1.65. At 1515 m and 1610 m, CBT could not be calculated due to the absence, or too low abundance of branched GDGTs with a cyclopentane moiety (i.e. Ib and IIb; Fig. 1). MBT values vary between 0.21 and 0.83. The highest values are found at the lower part of the slope in the shrub and grass vegetation zone (1000–1600 m), above which the MBT values are lower, and remain relatively constant along the rest of the slope.

The variable CBT and MBT values along the altitude gradient suggest that the branched GDGT distribution is influenced by changes in MAT and soil pH. The CBT index shows a linear relation with the measured soil pH (r^2=0.72, n=34; Fig. 3), and this relation is not significantly different from the global CBT-pH relationship reported by Weijers et al. (2007c), neither for the slope (homogeneity of slopes test: df=1,144, F=0.01, P=0.92), nor for the intercept (ANCOVA: df=1,145, F=0.36, P=0.55). A comparison of the calculated soil pH, derived from the CBT index and Eq. (4), and the measured soil pH, varying from 7.9 at the lower slope to 4.4 at higher elevation (Table 2), shows no significant differences (paired t-test: $t(33)=-0.072$, P=0.94), suggesting that changes in soil pH indeed influence the distribution of branched GDGTs, and that the CBT index is a suitable tool to detect those changes.

MAT values along the slope were calculated based on the MBT and CBT indices and Eq. (4). MBT/CBT-derived MATs range from 20.9°C at the lower slope (1220 m) to

−3.1°C at the upper slope (3209 m), and show a linear decrease with altitude (r^2=0.55, n=34; Fig. 4). The temperature lapse rate based on the MBT/CBT-derived MAT values is −5.9±0.9°C/1000 m for Mt. Gongga. This calculated lapse rate is identical to the temperature lapse rate of −6.0°C/1000 m based on the weather station data. Nevertheless, there is a relatively large scatter in the MBT/CBT-derived MAT relationship with altitude, larger than observed for Mt. Kilimanjaro (Sinninghe Damseé et al., 2008). Possibly, other factors than pH or temperature, like soil type or the length of the growing season, have caused the relatively large scatter for this altitude gradient. This suggests that estimations of temperature are associated with relatively large uncertainties, which makes this proxy less suitable for accurate paleoelevation studies in this area.

4 Implications and conclusions

Our results for the δD_{wax} in soils of Mt. Kilimanjaro suggest that caution should be taken in deriving a reference record for paleoelevation reconstructions based on *n*-alkane δD values for an altitude transect that experiences large varieties in the amount of precipitation. Likely, the relatively high amounts of precipitation in the middle montane belt cause a relative depletion in D of the plant wax *n*-alkanes, and therefore mask the relation between δD_{wax} and altitude (r^2=0.03, n=16; Fig. 2b) required for a paleoelevation proxy. Indeed, the calculated "δD-lapse rate" along Mt. Kilimanjaro would be 2.6±4.2‰/1000 m, suggesting that, due to both the large error and the absence of a linear relation, δD_{wax} is unlikely to be useful at this location. In contrast, the MBT/CBT temperature proxy at Mt. Kilimanjaro, which is not influenced by precipitation, shows a good linear relation with altitude (r^2=0.77, n=16; Sinninghe Damsté et al., 2008), although the MBT/CBT-based temperature lapse rate (−6.9±1.0°C/1000 m) is somewhat higher than the measured lapse rate (−5.3±0.1°C/1000 m; Hemp 2006a, b). In case of Mt. Gongga, *n*-alkane δD values relate linearly with altitude (Jia et al., 2008), thereby providing a fairly good proxy to estimate "δD-lapse rate" (17.7±1.7‰/1000 m). Although the MBT/CBT-based MAT estimates also shows a linear relation with altitude,

BGD
6, 8609–8631, 2009

and provides a temperature lapse rate that resembles the measured lapse rate (respectively −5.8°C and −6.0°C/1000 m), there is a large degree of scatter in this correlation.

Thus, it seems that for the two studied mountains, neither potential paleoelevation proxy is working perfectly. However, the combination of soil *n*-alkane δD values and the MBT/CBT temperature proxy may be a suitable alternative for the more traditional $\delta^{18}O$ based paleoelevation reconstructions. The combination of both proxies is easily made, as they can be determined from the same lipid extract, yet they are based on fundamentally different principles. Similar paleoelevation estimates from both proxies would yield increased confidence. Compared to the more traditional $\delta^{18}O$ based reconstructions, it should then be possible to obtain higher resolution records, as plant growth and adaptations in bacterial cell membranes are relatively fast processes. Furthermore, branched GDGTs and *n*-alkanes are relatively more resistant to diagenesis than soil carbonate, and paleoelevation studies may also be performed in areas where no carbonates or other minerals are present.

Acknowledgements. We thank D. Verschuren (University of Gent, Belgium) for logistic support and helpful discussions, and A. Hemp (University of Bayreuth, Germany) for hospitality and guidance during fieldwork in Tanzania. This work was partially performed as part of the ESF Euroclimate project Challacea, financially supported by the Dutch Organization for Scientific Research (NWO). This is publication number DW-2009-5002 of the Darwin Center for Biogeosciences, which partially funded this project.

References

Bowen, G. J. and Revenaugh, J.: Interpolating the isotopic composition of modern meteoric precipitation, Water Resour. Res., 39, SWC9-1–SWC9-13, 2003.

Bowen, G. J.: The Online Isotopes in Precipitation Caclulator, version 2.2., http://www.waterisotopes.org, last access: August 2009.

Chikaraishi, Y. and Naraoka, H.: Compound-specific δD–$\delta^{13}C$ analyses of *n*-alkanes extracted from terrestrial and aquatic plants, Phytochemistry, 63, 361–371, 2003.

Dansgaard, W.: Stable isotopes in precipitation, Tellus, XVI, 436–468, 1964.

Dettman, D. L. and Lohmann, K. C.: Oxygen isotope evidence for high-altitude snow in the Laramide Rocky Mountains of North America during the late Cretaceous and Paleogene, Geology, 28, 243–246, 2000.

Garzione, C. N., Dettman, D. L., and Horton, B. K.: Carbonate oxygen isotope paleoaltimetry: evaluating the effect of diagenesis on paleoelevation estimates for the Tibetan plateau, Palaeogeogr. Palaeocl., 212, 119–140, 2004.

Hemp, A.: Continuum or zonation? Altitudinal gradients in the forest vegetation of Mt. Kilimanjaro, Plant Ecol., 184, 27–42, 2006a.

Hemp, A.: Vegetation of Kilimanjaro: hidden endemics and missing bamboo, Afr. J. Ecol., 44, 305–328, 2006b.

Huguet, C., Hopmans, E. C., Febo-Ayala, W., Thompson, D. H., Sinninghe Damsté, J. S., and Schouten, S.: An improved method to determine the absolute abundance of glycerol dibiphytanyl glycerol tetraether lipids, Org. Geochem., 37, 1036–1041, 2006.

Jia, G., Wei, K., Chen, F., and Peng, P.: Soil *n*-alkane δD vs. altitude gradients along Mount Gongga, China, Geochim. Cosmochim. Acta, 72, 5165–5174, 2008.

Morrill, C. and Koch, P. L.: Elevation or alteration? Evaluation of isotopic constraints on paleoaltitudes surrounding the Eocene Green River Basin, Geology, 30, 151–154, 2002.

Pedentchouk, N., Sumner, W., Tipple, B., and Pagani, M.: $\delta^{13}C$ and δD compositions of *n*-alkanes from modern angiosperms and conifers: an experimental set up in central Washington State, USA, Org. Geochem., 39, 1066–1071, 2008.

Pedentchouk, N., Wagner, T., Jones, W., Pellegrini, M., Brugnoli, E., Lauteri, M., Pollegioni, P., and Behling, H.: Comparison of $\delta^{13}C$ and δD values of *n*-alkanes from angiosperms and gymnosperms in western Europe, Geochim. Cosmochim. Acta, 71, A770, 2007.

Poage, M. A. and Chamberlain, C. P.: Empirical relationships between elevation and the stable isotope composition of precipitation and surface waters: considerations for studies of paleoelevation change, Am. J. Sci., 301, 1–15, 2001.

Rao, Z., Zhu, Z., Jia, G., Henderson, A. C. G., Xue, Q., and Wang, S.: Compound specific δD values of long chain *n*-alkanes derived from terrestrial higher plants are indicative of the δD of meteoric waters: evidence from surface soils in eastern China, Org. Geochem., 40, 922–930, 2009.

Rietti-Shati, M., Yam, R., Karlen, W., and Shemesh, A.: Stable isotope composition of tropical high-altitude fresh-waters on Mt. Kenya, Equatorial East Arfica, Chem. Geol., 166, 341–350, 2000.

Risi, C., Bony, S., and Vimeux, F.: Influence of convective processes on the isotopic composition (δ^{18}O and δD) of precipitation and water vapor in the tropics: 2. Physical interpretation of the amount effect. J. Geophys. Res.-Atmos., 113, D19306-1–D19306-12, 2008a.

Risi, C., Bony, S., Vimeux, F., Descroix, L., Ibrahim, B., Lebreton, E., Mamadou, I., and Sultan, B.: What controls the isotopic composition of the African monsoon precipitation? Insights from event-based precipitation collected during the 2006 AMMA field campaign, Geophys. Res. Lett., 35, L24808-1–L24808-6, 2008b.

Rommerskirchen, F., Plader, A., Eglinton, G., Chikaraishi, Y., and Rullkötter, J.: Chemotaxonomic significance of distribution and stable carbon isotopic composition of long-chain alkanes and alkan-1-ols in C_4 grass waxes, Org. Geochem., 37, 1303–1332, 2006.

Rowley, D. B. and Garzione, C. N.: Stable isotope-based paleoaltimetry, Annu. Rev. Earth Pl. Sc., 35, 463–508, 2007.

Rozanski, K. and Araguás Araguás, L.: Spatial and temporal variability of stable isotope composition of precipitation over the South American continent, Bulletin de l'Institut Français d'Études Andines, 24, 379–390, 1995.

Rozanski, K., Araguás-Araguás, L., and Gonfiantini, R.: Relation between long-term trends of O^{18} isotope composition of precipitation and climate, Science, 258, 981–985, 1992.

Sachse, D., Radke, J., and Gleixner, G.: Hydrogen isotope ratios of recent lacustrine sedimentary *n*-alkanes record modern climate variability, Geochim. Cosmochim. Acta, 68, 4877–4889, 2004.

Sauer, P. E., Eglinton, T. I., Hayes, J. M., Schimmelmann, A., and Sessions, A. L.: Compound-specific D/H ratios of lipid biomarkers from sediments as a proxy for environmental and climatic conditions. Geochim. Cosmochim. Acta, 65, 213–222, 2001.

Schouten, S., Eldrett, J., Greenwood, D. R., Harding, I., Baas, M., and Sinninghe Damsté, J. S.: Onset of long-term cooling of Greenland near the Eocene-Oligocene boundary as revealed by branched tetraether lipids, Geology, 36, 147–150, 2008.

Schouten, S., Huguet, C., Hopmans, E. C., Kienhuis, M. V. M., and Sinninghe Damsté, J. S.: Analytical methodology for TEX_{86} paleothermometry by high-performance liquid chromatography/atmospheric pressure chemical ionization-mass spectrometry, Anal. Chem., 79, 2940–2944, 2007.

Sessions, A. L., Burgoyne, T. W., Schimmelmann, A., and Hayes, J. M.: Fractionation of hydrogen isotopes in lipid biosynthesis, Org. Geochem., 30, 1193–1200, 1999.

Sinninghe Damsté, J. S., Hopmans, E. C., Pancost, R. D., Schouten, S., and Geenevasen,

J. A. J.: Newly discovered non-isoprenoid glycerol dialkyl glycerol tetraether lipids in sediments, Chem. Commun., 17, 1683–1684, 2000.

Sinninghe Damsté, J. S., Ossebaar, J., Schouten, S., and Verschuren, D.: Altitudinal shifts in the branched tetraether lipid distribution in soil from Mt. Kilimanjaro (Tanzania): Implications for the MBT/CGT continental palaeothermometer, Org. Geochem., 39, 1072–1076, 2008.

Smith, F. A. and Freeman, K. H.: Influence of physiology and climate on δD of leaf wax *n*-alkanes from C_3 and C_4 grasses, Geochim. Cosmochim. Acta, 70, 1172–1187, 2006.

Thomas, A.: The climate of the Gongga Shan range, Sichuan Province, PR China, Arctic Alpine Res., 29, 226–232, 1997.

Thomas, A.: Overview of the geoecology of the Gongga Shan range, Sichuan province, China, Mt. Res. Dev., 19, 17–30, 1999.

Vimeux, F., Gallaire, R., Bony, S., Hoffmann, G., and Chiang, J. C. H.: What are the climate controls on δD in precipitation in the Zongo Valley (Bolivia)? Implications for the Illimani ice core interpretation, Earth Planet Sci. Lett., 240, 205–220, 2005.

Weijers, J. W. H., Schefuß, E., Schouten, S., and Sinninghe Damsté, J. S.: Coupled thermal and hydrological evolution of tropical Africa over the last deglaciation, Science, 315, 1701–1704, 2007a.

Weijers, J. W. H., Schouten, S., Hopmans, E. C., Geenevasen, J. A. J., David, O. R. P., Coleman, J. M., Pancost, R. D., and Sinninghe Damsté, J. S.: Membrane lipids of mesophilic anaerobic bacteria thriving in peats have typical archaeal traits, Environ. Microbiol., 8, 648–657, 2006.

Weijers, J. W. H., Schouten, S., Sluijs, A., Brinkhuis, H., and Sinninghe Damsté, J. S.: Warm arctic continents during the Palaeocene-Eocene thermal maximum, Earth Planet Sci. Lett., 261, 230–238, 2007b.

Weijers, J. W. H., Schouten, S., van den Donker, J. C., Hopmans, E. C., and Sinninghe Damsté, J. S.: Environmental controls on bacterial tetraether membrane lipid distribution in soils, Geochim. Cosmochim. Acta, 71, 703–713, 2007c.

Zhong, X., Zhang, W., and Luo, J.: The characteristics of the mountain ecosystem and environment in the Gongga Mountain region, AMBIO, 28, 648–654, 1999.

Table 1. δD values for soil *n*-alkanes and precipitation (‰), carbon preference index, and average chain length of soil *n*-alkanes along the southeastern slope of Mt. Kilimanjaro.

Altitude	Soil *n*-alkane						
(m)	$\delta D_{C_{29}} \pm SD$[a]	$\delta D_{C_{31}} \pm SD$	$\delta D_{C_{33}} \pm SD$	δD_{wax}[b]	δD_p[c]	CPI[d]	$ACL_{C27-C35}$[e]
1727	−114±6	−118±12	−129±6	−119.4	−23	5.9	31.9
1822	−135±2	−125±0	−129±4	−128.2	−24	7.5	31.5
1967	−156±1	−138±1	−134±2	−142.6	−27	12.1	31.1
2068	−152±0	−144±2	−137±2	−145.9	−28	11.2	30.7
2124	−150±1	−140±3	−139±1	−142.7	−29	11.0	30.7
2239	−154±1	−136±0	−130±2	−142.0	−30	11.9	30.8
2346	−152±1	−144±1	−144±1	−147.2	−32	11.4	30.4
2464	−151±2	−147±1	−140±1	−147.2	−34	13.6	30.2
2578	−139±3	−134±1	−118±1	−133.6	−35	5.5	30.7
2652	−144±3	−149±1	−137±3	−146.1	−36	13.4	31.4
2764	−149±4	−143±1	−121±0	−140.8	−38	15.8	31.1
2885	−138±2	−136±2	−125±2	−132.9	−40	9.8	31.4
2999	−144±4	−143±1	−135±0	−139.9	−41	13.5	31.9
3070	−154±3	−133±4	−124±5	−132.4	−42	14.1	32.1
3157	−143±2	−138±3	−132±4	−137.2	−43	14.7	31.5
3245	−151±0	−143±1	−134±1	−140.4	−45	9.2	32.0

[a] Standard deviation of at least duplicate measurements
[b] Weighed means of C_{29}, C_{31}, and C_{33} *n*-alkanes
[c] Modeled precipitation δD along Mt. Kilimanjaro
[d] Carbon Preference Index (CPI), with $CPI=1/2*((\Sigma(X_i+X_{i+2}+\ldots+X_n)/\Sigma(X_{i-1}+X_{i+1}+\ldots+X_{n-1}))+(\Sigma(X_i+X_{i+2}+\ldots+X_n)/\Sigma(X_{i+1}+X_{i+3}+\ldots+X_{n+1})))$, with i=25 and n=33
[e] Average chain length (ACL) of C_{27}–C_{35} *n*-alkanes

BGD
6, 8609–8631, 2009

Table 2. Soil pH, branched GDGT concentrations, MBT/CBT values, CBT-derived pH, and MBT/CBT-derived MAT for soils along the eastern slope of Mt. Gongga.

Altitude (m)	Soil pH	Total branched GDGTs (μg/g dry weight soil)	CBT	MBT	CBT-derived pH	MBT/CBT-derived MAT (°C)
1180	7.9	0.01	0.72	0.43	6.9	8.7
1220	7.3	0.14	0.61	0.65	7.2	20.9
1515	n.d.[a]	0.62	–[b]	0.83	–	–
1610	7.8	0.01	–	0.25	–	–
1645	7.5	0.42	0.12	0.38	8.4	11.9
1740	6.7	0.01	0.37	0.49	7.8	15.0
1800	7.1	0.72	0.33	0.32	7.9	6.6
1850	7.5	0.15	0.26	0.33	8.1	7.7
1915	6.9	1.17	0.72	0.55	6.9	14.5
1973	7.7	2.69	0.06	0.23	8.6	5.0
2005	7.5	1.30	0.63	0.40	7.1	7.9
2115	7.1	0.46	0.03	0.23	8.7	5.2
2160	7.9	0.51	0.36	0.35	7.8	7.9
2220	6.6	0.26	0.79	0.37	6.7	4.8
2300	6.7	0.86	1.06	0.41	6.0	4.7
2350	6.9	1.28	0.66	0.36	7.0	5.8
2420	7.2	0.47	0.63	0.28	7.1	1.9
2470	7.9	0.66	0.58	0.26	7.2	1.5
2540	7.8	0.13	0.23	0.24	8.1	3.7
2620	6.5	0.16	0.45	0.34	7.6	6.5
2742	4.4	2.86	1.47	0.67	4.9	13.8
2764	5.9	2.68	1.26	0.44	5.4	4.1
2808	5.0	5.29	1.32	0.57	5.3	10.1
2920	5.2	1.22	1.40	0.39	5.1	0.5
2960	7.2	0.67	0.60	0.34	7.2	5.3
3049	4.5	1.96	1.56	0.48	4.7	3.1
3065	6.4	0.34	1.10	0.31	5.9	−1.0
3119	5.6	0.49	1.38	0.39	5.1	0.5
3140	4.9	0.61	1.65	0.57	4.4	7.2
3145	7.3	0.11	0.67	0.21	7.0	−1.8
3188	5.3	0.49	1.44	0.43	5.0	2.0
3209	5.0	0.24	1.44	0.33	5.0	−3.1
3518	4.4	4.69	1.50	0.44	4.8	2.0
3676	6.6	0.33	1.43	0.36	5.0	−1.7
3769	6.3	1.93	1.59	0.37	4.6	−2.5
3819	5.0	1.94	1.48	0.38	4.9	−0.8

[a] not determined
[b] could not be calculated

BGD
6, 8609–8631, 2009

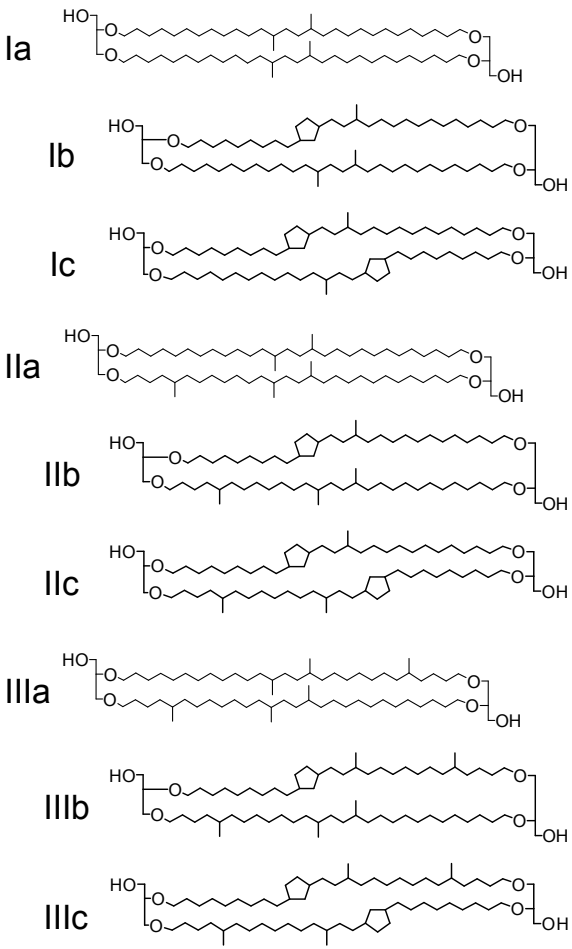

Fig. 1. Molecular structures of branched GDGTs.

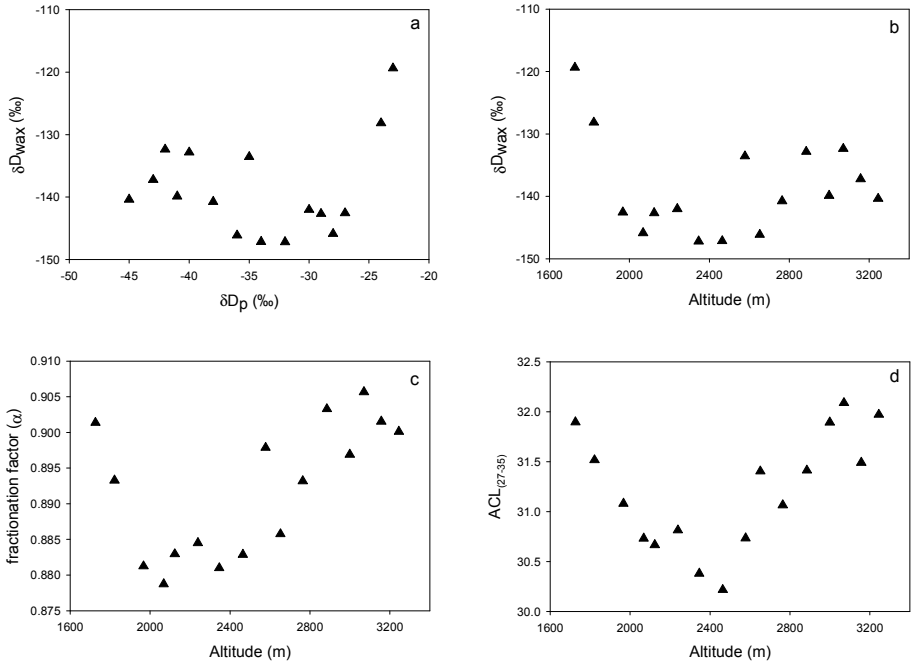

Fig. 2. Relations of δD_{wax} with **(a)** δD_p and **(b)** altitude in ‰ versus VSMOW, and altitudinal changes in **(c)** isotopic fractionation factor α and **(d)** the average chain length (ACL) for soil *n*-alkanes C_{27}–C_{35} along the southeastern slope of Mt. Kilimanjaro.

BGD
6, 8609–8631, 2009

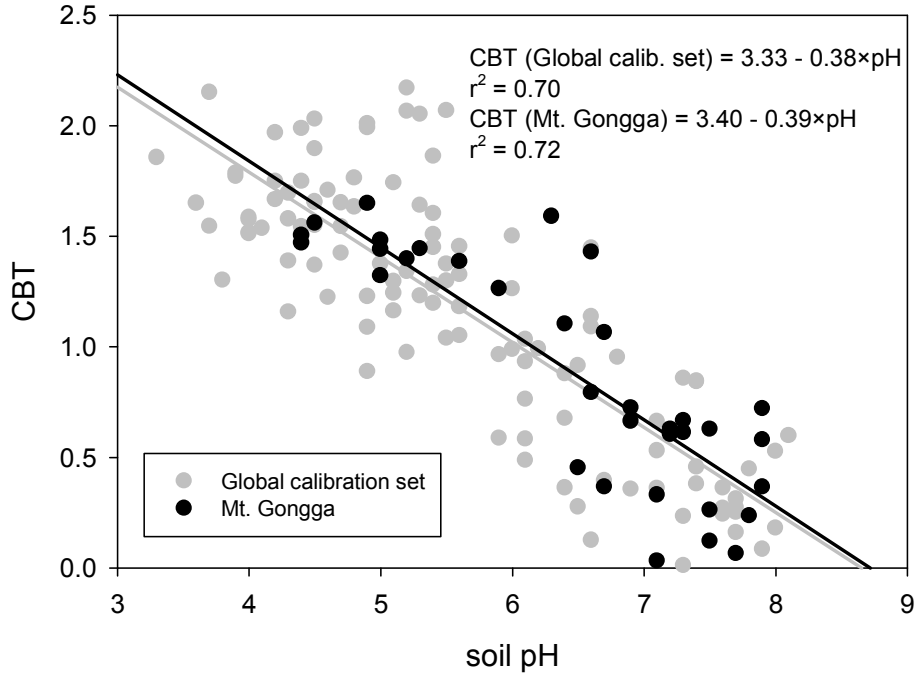

Fig. 3. Cross plot of the CBT index vs. measured soil pH for the soils along the eastern slope of Mt. Gongga (black) and for the global soil calibration set of Weijers et al. (2007c) (grey).

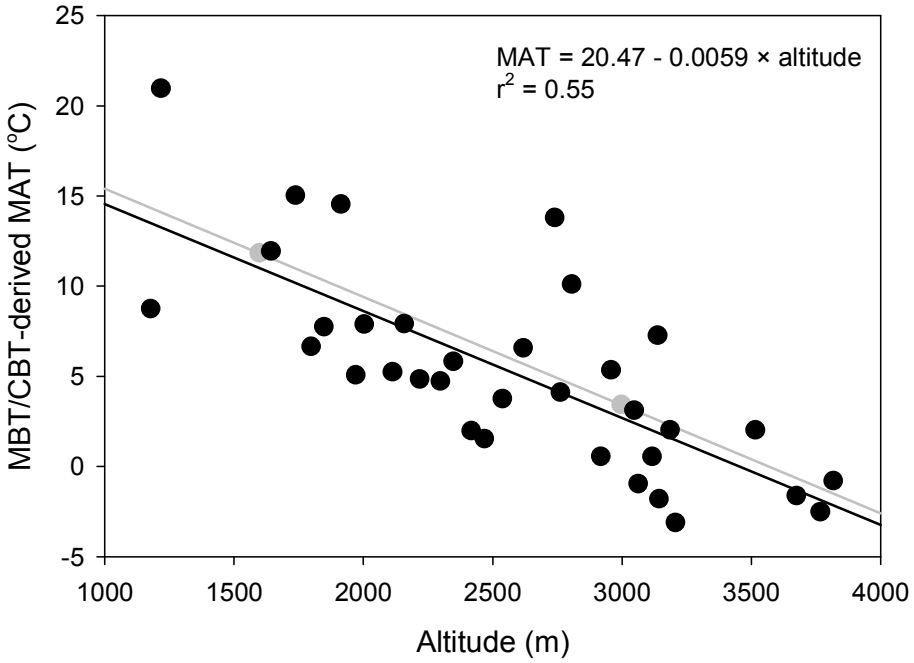

Fig. 4. Relations of MBT/CBT-derived MATs (black) and weather station data (grey) with altitude along the eastern slope of Mt. Gongga.